

Non-Isothermal Approach to Isokinetic Crystallization Processes: Application to the Nanocrystallization of HITPERM Alloys.

J. S. Blázquez, C. F. Conde, A. Conde*

*Departamento de Física de la Materia Condensada. Instituto de Ciencia de Materiales, CSIC
Universidad de Sevilla. Apartado 1065, 41080-Sevilla, Spain.*

Keywords: crystallization, phase transformation kinetics, nanocrystalline microstructure.

Abstract

A new approach is proposed for the study of crystallization processes under the hypothesis of isokinetic behavior. From a direct extension of the Avrami theory to non-isothermal regimes, an expression of the local Avrami exponent as a function of the crystalline volume fraction is obtained from a single DSC run performed at a constant heating rate and a raw estimation of the activation energy (a variation of the activation energy value between 3 and 5 eV produces a change on the Avrami exponent smaller than ± 0.1). This approximation was applied to the nanocrystallization process of a FeCoNbB(Cu) alloy series and the results found are in good agreement with previous isothermal analysis on the same alloys. The kinetics is characterized by an initial Avrami exponent close to unity, which decreases down to values below 0.5 as the crystalline volume fraction increases.

*Corresponding author: Prof. A. Conde

Departamento de Física de la Materia Condensada. Universidad de Sevilla.

Apartado 1065, 41080 Sevilla (Spain).

Phone: (34) 95 455 28 85

Fax: (34) 95 461 20 97

E-mail: conde@us.es

1. Introduction

Nowadays, an important effort is devoted to the research of metastable structures. A strong enhancement of different physical properties is found for several metastable structures with respect to their corresponding one in the thermodynamical equilibrium state. For example, in Fe-based alloys amorphous and nanocrystalline microstructures improve several orders of magnitude some properties of both soft and hard magnetic materials depending on the composition [1-4] and quasicrystalline and nanocrystalline structures strongly improve the mechanical properties of Al-base alloys [5].

Metastable structures are not in thermodynamic equilibrium and, therefore, they can spontaneously evolve to new more stable structures, although sometimes still metastable ones. After these transformation processes, the materials usually modify their properties. Besides, interesting metastable structures can be produced in a controlled way from the evolution of a previous metastable but less stable structure: for example, the controlled heat treatment of certain amorphous alloys can produce nanocrystalline or quasicrystalline structures or just structurally relaxed amorphous alloys in which the desired physical properties are strongly enhanced with respect to the amorphous precursor [1-5]. Therefore, kinetics of transformation must be considered as a very important task, which gives information relative to the stability and thus the applicability of these materials, as well as supports the parameters necessary to control the production of a desired microstructure.

The evolution of the metastable structures can be studied in both isothermal and non-isothermal processes. Non-isothermal experiments in relation to isothermal ones have the advantage of an easier and faster performance, as well as a smaller noise to signal ratio for kinetic experiments. However, the range of applicability of the different non-isothermal methods of analysis must be considered, because most of them were obtained as approximations of theories which theoretical applicability is on isothermal regimes. In this work, a new non-isothermal approach is proposed to study the primary crystallization of amorphous alloys as an extension of the Johnson-Mehl-Avrami-Kolmogorov theory of crystallization [6-10]. A comparison is performed between this new method and several non-isothermal approaches,

widely used for the study of non-isothermal crystallization kinetics. The limits of applicability of different methods as well as the advantages of this new method with respect to others found in the literature are emphasized. Finally, an application of the proposed method to experimental data is performed studying the kinetics of the nanocrystallization process of a FeCoNbB(Cu) alloy series by different non-isothermal methods and comparing the obtained results with previous ones from isothermal kinetics [11].

2. Non-isothermal kinetic models.

Crystallization kinetics of metallic glasses is usually studied in the frame of the Johnson-Mehl-Avrami-Kolmogorov (JMAK) theory [6-10], which can be expressed by the so-called JMAK equation:

$$X = 1 - \exp[-\{k(t-t_0)\}^n] \quad (1)$$

where k is the frequency factor, t the time, t_0 the induction time, n the Avrami exponent and X the effective crystalline volume fraction, normalized to the value at the end of the process. The JMAK theory was developed for isothermal processes, however, some approximations have been done for extending it to non-isothermal transformations.

Nakamura et al. [12,13] generalized JMAK equation to non-isothermal processes under the approximation of isokinetic behavior. This approximation implies that the crystallization process is independent of the thermal history of the sample. In Nakamura equation, the dependence of X with temperature, T , and time is given by:

$$X = 1 - \exp\left\{-\left[\int_{t_0}^t k(T) dt\right]^n\right\} \quad (2)$$

For isothermal processes, at temperature T_{ISO} , this equation yields directly the JMAK equation (1), being constant $k(T_{ISO}) = k$. On the other hand, in the case of a constant heating rate $dT/dt = \beta$, it is possible to write:

$$X = 1 - \exp\left\{-\left(1/\beta^n\right)\left[\int_{T_0}^T k(T) dT\right]^n\right\} \quad (3)$$

which can be written as:

$$X = 1 - \exp\left\{-\frac{Z(T)}{\beta^n}\right\} \quad (4)$$

where

$$Z(T) = \left[\int_{T_0}^T k(T) dT \right]^n \quad (5)$$

being $Z(T)$ the crystallization function. Expression (4), known as the Ozawa equation [14], allows to obtain the Avrami exponent as the slope of the plot of $\text{Ln}[-\text{Ln}[1-X(T)]]$ vs $\text{Ln}[1/\beta]$ for a selected temperature T and different β values. Under this approximation, it is worth noticing that, at a given temperature for different scanning rates the process might be in a different stage of development. Therefore, in this approach, kinetic parameters, as Avrami exponent and activation energy (Q), are considered independent of X .

From Ozawa theory it is also possible to obtain a simple expression for Q if an Arrhenius law is used to describe the evolution of $Z(T)$ [15]. Thus, expression (4) can be rewritten as:

$$\text{Ln}[-\text{Ln}[1-X]] = \text{Ln}[Z_0] - Q/RT - n\text{Ln}[\beta] \quad (6)$$

and for a constant value of X , achieved at different temperatures, $T(X_0)$, depending on β , yields:

$$d(\text{Ln}[\beta])/d(1/T(X_0)) = -Q/(nR) \quad (7)$$

Besides these approaches which give a local information of kinetic parameters $n(X)$ and $Q(X)$, there are different approximations of the JMAK equation for non-isothermal processes from which it is possible to obtain averaged values of the kinetic parameters. Most of them use the hypothesis of maximum transformation rate at the peak temperature (T_p), being $(d^2X/dt^2)_p = 0$. Thus, by different representations of the parameters at T_p it is possible to obtain average values of Q and in some cases of n . Among these methods the Kissinger [16,17], Augis-Bennett [18] and Gao-Wang [19] methods are found. Although the former is the most widely used, its theoretical validity for describing crystallization of amorphous alloys has been

questioned by some authors [20,21]. The Kissinger method can be summarized in the expression:

$$\frac{d\left(\ln\left[\beta/T_p^2\right]\right)}{d\left(1/T_p\right)} = -\frac{Q}{R} \quad (8)$$

On the other hand, the Augis-Bennett method considers the influence of the onset temperature and yields the expression:

$$\frac{d\left(\ln\left[\beta/(T_p - T_o)\right]\right)}{d\left(1/T_p\right)} = -\frac{Q}{R} \quad (9)$$

Finally, the Gao-Wang method gives two expressions, which allow calculating both Q :

$$\frac{d\left(\ln\left[(dX/dt)_p\right]\right)}{d\left(1/T_p\right)} = -\frac{Q}{R} \quad (10)$$

and the Avrami exponent:

$$(dX/dt)_p = 0.37n\beta Q/(RT_p^2) \quad (11)$$

Therefore, from plots of $\ln[\beta/T_p^2]$, $\ln[\beta/(T_p - T_o)]$ and $\ln[(dX/dt)_p]$ versus $1/T_p$ for different values of β (Kissinger, Augis-Bennett and Gao-Wang plots, respectively), it is possible to estimate Q values. It is worthy to note that the information obtained from these three methods is somehow averaged in temperature, due to the change of T_p and T_o with β . However, the value of X at T_p is, in a good approximation, independent of β and, therefore, it can be considered that the values of the kinetic parameters obtained by these methods correspond to the value of X at the peak temperature, $X(T_p)$.

An important difference between the Ozawa method and the previous ones is that the Ozawa method allows to select different values of X , and not only that of T_p . It must be taken into account that, in Ozawa theory, kinetic parameters are supposed to be constant during the whole crystallization process. However, we could interpret expression (7) as a dependence on T of the kinetic parameters only through X . That means there is no dependence on the thermal history of the sample but on the crystallization stage, it is said, in the frame of isokinetic approximation used by the Nakamura theory.

3. Direct extension of JMAK equation to non-isothermal kinetic regimes.

The method proposed in this work consists on a direct extension of the JMAK equation to non-isothermal processes. Although the idea seems to be quite simple and raw, its validity and limitations will be demonstrated. If Eq.(1) is directly used for non-isothermal treatments with a constant heating rate, it should be taken into account that $t-t_0 = (T-T_0)/\beta$, where T_0 is the temperature at the crystallization onset. Therefore, it can be written:

$$X = 1 - \exp[-\{k'(T-T_0)/\beta\}^n] \quad (12)$$

where k' is a new frequency factor.

The relationship between the different equations can be observed through the Nakamura equation. Assuming an Arrhenius dependence of k' with T :

$$k' = k'_0 \exp[-Q/RT] \quad (13)$$

where k'_0 is a constant, Q is the activation energy and R is the gas constant and comparing equation (3), (4) and (12), it is possible to write:

$$k'_0 \exp[-Q/RT](T - T_0) = \int_{T_0}^T k(T) dT = Z(T)^{1/n} \quad (14)$$

$$k(T) = k'_0 \{1 + (T-T_0)Q/RT^2\} \exp[-Q/RT] \quad (15)$$

Expression (15) is a more complicated form than the simple Arrhenius law:

$$k(T) = k_0 \exp[-Q/RT] \quad (16)$$

normally used to describe the temperature dependence of some kinetic parameters, as the frequency factor and the induction time. In our case, to simplify the expressions, Arrhenius law was used to describe the behavior of the parameter k' .

In the case of JMAK equation (1), for isothermal processes the local Avrami exponent at a selected value of X , $n(X)$, can be obtained from the slope of $\text{Ln}[-\text{Ln}[1-X]]$ vs $\text{Ln}[t-t_0]$:

$$n(X) = \frac{d(\text{Ln}[-\text{Ln}(1-X)])}{d(\text{Ln}[t-t_0])} \quad (17)$$

but, in the case of non-isothermal transformations the dependency of k' with T must be considered. Therefore, the expression (17) would be:

$$\frac{d(\text{Ln}[-\text{Ln}(1-X)])}{d(\text{Ln}[(T-T_o)/\beta])} = n \left\{ 1 + \frac{d(\text{Ln}(k'))}{d(\text{Ln}[(T-T_o)/\beta])} \right\} = n \left\{ 1 + \frac{Q}{RT} \left(1 - \frac{T_o}{T} \right) \right\} \quad (18)$$

It is clear that (18) reduces to (17) for isothermal treatments, where $T = T_o$ is constant. From (18) it will be easy to obtain $n(X)$.

The proposed approximation shows two main advantages with respect to the Ozawa approach:

First, in Ozawa approximation, the local Avrami exponent, $n(T)$, is calculated as a function of T for different values of β and, therefore, it is implicitly assumed that the process is independent of X , which value depends on β for a given temperature. However, in the direct extension of JMAK to non-isothermal processes, the local Avrami exponent, $n(X)$, is calculated as a function of X , independently of β .

Second, an important characteristic of the direct extension of JMAK to non-isothermal processes is that, as for isothermal cases, n can be obtained directly from (18) using only one run, at a single value of the constant heating rate, β . However, it will be necessary to have an estimation of the activation energy value which, for example, could be obtained from literature data. In fact, as it will be shown below, the main results obtained using the direct extension of JMAK equation to non-isothermal regimes are not significantly affected even by an important change of Q value.

4. Application to nanocrystallization process of FeCoNbB(Cu) alloys.

The method proposed above has been applied to the nanocrystallization process of a FeCoNbB(Cu) alloy series. Amorphous ribbons, about 20 μm in thickness, of nominal composition $\text{Fe}_{78-x}\text{Co}_x\text{Nb}_6\text{B}_{16-y}\text{Cu}_y$ ($x = 18, 39, 60$; $y = 0, 1$) were prepared by a single wheel melt spinning technique. Differential scanning calorimetry (DSC) scans of as-cast samples were performed in a Perkin-Elmer DSC7 at different heating rates (2.5, 5, 10, 20, 40 and 80 K/min).

Transition temperatures of Pb and CrO₃K standards were used for the calibration of the calorimeter and correction of thermal lag in the DSC scans. Values of X were calculated from the normalized integration of the dH/dt signal after subtraction of the baseline. In the case of the alloy with 18 at. % of Co and with Cu heated at 80 K/min, the nanocrystallization process was not completed in the temperature range available for the DSC7 (up to 1000 K). Therefore, this rate was discarded in the analyses that involve a good knowledge of the baseline.

Figure 1 shows, as an example, DSC plots for Fe₆₀Co₁₈Nb₆B₁₆ amorphous alloy for the nanocrystallization process at different heating rates. As β increases, the width of the nanocrystallization peak decreases and T_p shifts to higher values (as it is expected for a thermally activated process).

As it was pointed above, isokinetic behavior was a requirement for applying Nakamura equation. Instantaneous nucleation would fulfill this requirement. For the nanocrystallization of FeCoNbB(Cu) alloys, isothermal studies showed that nucleation is mainly restricted to the initial stages of the process [11]. In fact, in the case of the alloys with Cu, clusters of this element, formed previous to the onset of nanocrystallization, act as heterogeneous nucleation centers for the α -FeCo nanocrystals [22], supporting the instantaneous nucleation approximation. On the other hand, in the case of Cu free alloys, the presence of quenched in nuclei might be invoked.

In the aim of a systematic comparison between the direct extension of JMAK and the other methods, Q values were obtained by different methods. Figure 2 shows the Kissinger (above), Augis-Bennett (center) and Gao-Wang (below) plots for the studied alloys. The linear regime is well reproduced in all the three methods for all the studied samples and, as can be observed in Table I, Q values from the three methods are in a good agreement for every alloy. The obtained values of Q are similar to those found in other NANOPERM and HITPERM alloys [23-25].

Once the Q value has been calculated, it is possible to use expression (18) to obtain the local Avrami exponent, for the nanocrystallization process. Figure 3 presents plots of the local Avrami exponent, $n(X)$, for the Fe₆₀Co₁₈Nb₆B₁₆ alloy obtained from DSC scans at different

scanning rates using the Q value obtained from the Kissinger method. As can be observed, all the curves are nearly collapsing in a single one, in agreement with the expected independent behavior of $n(X)$ with β derived from the isokinetic assumption. The observed differences are quite small considering the uncertainty of the baseline, an inherent problem to the DSC analyses of transformations extended to a broad temperature range (~ 100 - 150 K in our case). Figure 4 presents the $n(X)$ curves obtained for the different alloys heated at $\beta = 10$ K/min.

To apply the approximation proposed in this work and summarized in equation (18), first, it is necessary to estimate Q . This estimation can be obtained from literature data. For example, in the case of nanocrystallization processes of α -Fe phase, Q ranges from 3.3 to 4.5 eV [1]. Figure 5 shows, for the $\text{Fe}_{60}\text{Co}_{18}\text{Nb}_6\text{B}_{16}$ alloy heated at 20 K/min, plots of expression (18) in which the effect of this indetermination in the Q values can be observed. Even using that wide range of activation energie values (3 to 5 eV), the Avrami exponent shows a maximum dispersion of ± 0.1 , which decreases as the crystalline volume fraction increases.

Ozawa theory also allows to obtain a local value of n , but as a function of T (Figure 6). As pointed before, this method implicitly assumes that kinetic parameters, both n and Q , are independent of the crystallization stage (it is said independent of X), which is a strong restriction. However, for all the studied alloys a range of temperature at which $n(T)$ is nearly constant is found. This range corresponds to the long tails observed at high X values, after the peak temperature, in nanocrystallization DSC curves. At these tails, where the evolution of enthalpy, and thus of X , is slower is where the requirements of the Ozawa method are better fulfilled: the system being in a similar situation of strongly hindered, slow growth process at this temperature range, independently of the scanning rate. For a better understanding of the meaning of the temperature dependence of the Avrami exponent, $n(T)$, in the Ozawa approach, we can use the results obtained from expression (18). From each $n_i(X)$, obtained for every β_i value, it is easy to obtain a $n_i(T)$ through the relation $X(T)$ obtained by the normalized integration of the corresponding DSC signal. For the $\text{Fe}_{60}\text{Co}_{18}\text{Nb}_6\text{B}_{16}$ alloy, figure 7 shows $n(T)$ plots obtained for different heating rates through expression (18) and from the Ozawa method.

As it can be observed, the agreement is pretty good, specially for the temperature range at which $n(T)$ is constant. In fact, along this temperature region, all the plots present the same value of n and the Ozawa plots present the best linear fitting (as can be inferred from the error bars, smaller than the symbol size in this range).

The present results on non-isothermal treatments clearly show a slowing down kinetics (clear decrease of $n(X)$ values) as the crystalline volume fraction increases. The initial values are close to 1, in agreement with the values found for the first stages of nanocrystallization by isothermal analysis [11] and coherent with those values found from Gao-Wang approach [26] ascribed to early stages of nanocrystallization ($X < 0.33$). Other nanocrystalline systems also show this characteristic behavior [23,27]. It is worth noticing that these results are independent of the Q value used in expression (18), at least in the range $3 < Q < 5$ eV for the nanocrystallization process.

It will be interesting to estimate the effect of a deviation of Q from a constant behavior during the process, as this approximation has been assumed in Eq. (18). In fact, isothermal analysis for the alloys with the lowest Co content shows a decreasing tendency of $Q(X)$ as X increases and for the $\text{Fe}_{60}\text{Co}_{18}\text{Nb}_6\text{B}_{16}$ alloy, this evolution of $Q(X)$ is close to linearity [11]. Therefore, it is possible to use a simple variation law for $Q(X)$ in expression (18). As the analysis is performed for a fixed X , this extension of the model to a variable $Q(X)$ value does not affect the analysis. However, it must be taken into account that Eq.(15) would be modified due to the Q dependence on T through X . Therefore, this extension to a variable $Q(X)$ is only proposed in a qualitative way. Figure 8 shows the $n(X)$ plot for a linear variation of $Q(X)$, along with the plot for a constant Q value for the $\text{Fe}_{60}\text{Co}_{18}\text{Nb}_6\text{B}_{16}$ alloy. Results from isothermal analysis of this alloy for two different annealing temperatures are also shown for comparison. It can be observed that the use of linear decreasing of $Q(X)$ enhances the agreement between non-isothermal and isothermal analysis.

The decrease found in activation energy as X increases can be understood in terms of nucleation and growth processes. This $Q(X)$ behavior has been reported for the crystallization of metallic glasses and other amorphous systems [28-30] and even FINEMET alloys [31]. The

decrease of Q as X increases was ascribed to a lower value for the growth activation energy than that corresponding to the nucleation process. In fact, this would mean that nucleation is extended (although continuously decreasing and meanly concentrated at the early stages) during the whole nanocrystallization process, which would imply a deviation from instantaneous nucleation. However, this deviation only seems to affect slightly the values of $n(X)$, as can be inferred from the rather good agreement between the results from non-isothermal analysis performed at different scanning rates and those obtained from isothermal treatments. On the other hand, the composition of the remaining uncrystallized matrix may change as crystallization proceeds and this can lead to changes in the crystallization parameters.

The expression (18) could not be applied to the second crystallization stage observed in the studied alloys. In this case, the complexity of the transformation, which includes the crystallization of the residual amorphous matrix forming different new phases, the coarsening of part of the nanocrystalline α -FeCo phase and its partial recrystallization to fcc $(\text{FeCoNb})_{23}\text{B}_6$ phase [32] provokes that the requirement for an isokinetic behavior is not fulfilled.

5. Conclusions

On the basis of isokinetic behavior and through Nakamura equation, a direct extension of Avrami theory was developed to obtain an expression of the local Avrami exponent as a function of X . The $n(X)$ function can be obtained from a single DSC run performed at a constant heating rate and a raw estimation of the activation energy (an indetermination of Q value between 3 and 5 eV produces a change on Avrami exponent smaller than ± 0.1).

This approximation, was applied to the nanocrystallization process of FeCoNbB(Cu) alloys and the results found are in good agreement with previous isothermal analysis on the same alloys. The kinetics is characterized by an initial Avrami exponent close to unity, which decreases down to values below 0.5 as the crystalline volume fraction increases.

Acknowledgments

This work was supported by the Spanish Government and EU FEDER (Project MAT 2004-04618). J.S. Blázquez acknowledges a research contract from the Regional Government of Andalucía (Spain).

References

- [1] McHenry ME, Willard MA, Laughlin DE, Prog Mater Sci 1999; 44: 291
- [2] Hono K, Prog Mater Sci 2002; 47: 621
- [3] Inoue A, Mater Sci Eng A 1997; 226-228: 357
- [4] Herzer G, J Magn Magn Mater 1996; 157-158: 133
- [5] Inoue A, Prog Mater Sci 1998; 43: 365
- [6] Johnson WA, Mehl RF, Trans Am Inst Mining Met Engrs 1939; 135: 416
- [7] Avrami M, J Chem Phys 1939; 7: 1103
- [8] Avrami M, J Chem Phys 1940; 8: 212
- [9] Avrami M, J Chem Phys 1941; 9: 177
- [10] Kolmogorov AN, Bull Acad Sci USSR, Phys Ser 1937; 1: 355
- [11] Blázquez JS, Conde CF, Conde A, Appl Phys A 2003; 76: 571
- [12] Nakamura K, Watanabe K, Katayama K, Amano T, J Appl Polym Sci 1972; 16: 1077
- [13] Nakamura K, Katayama K, Amano T, J Appl Polym Sci 1973; 17: 1031
- [14] Ozawa T, Polymer 1971; 12: 150
- [15] Gogebakan M, Warren PJ, Cantor B, Mat Sci Eng A 1997; 226-228: 168
- [16] Kissinger HE, J Res Nat Bur Stand 1956; 57: 217
- [17] Kissinger HE, Anal Chem 1957; 29: 1702
- [18] Augis JA, Bennett JE, J Thermal Anal 1978; 13: 283
- [19] Gao YQ, Wang W, J Non-Cryst Solids 1986; 81: 129
- [20] Yinnon H, Uhlmann DR, J Non-Cryst Solids, 1983; 54: 253
- [21] Altúzar P, Valenzuela R, Mater Lett 1991; 11: 101
- [22] Zhang Y, Blázquez JS, Conde A, Warren PJ, Cerezo A, Mat Sci Eng A 2003; 353: 158
- [23] McHenry ME, Johnson F, Okumura H, Ohkubo T, Ramanan VRV, Laughlin DE, Scripta Mater 2003; 48: 881
- [24] Hsiao A, Turgut Z, Willard MA, Sellinger E, Laughlin DE, McHenry ME, Hasegawa R, Mat Res Soc Symp Proc 1999; 577: 551

- [25] Hsiao A, McHenry ME, Laughlin DE, Kramer MJ, Ashe C, Ohkubo T, IEEE Trans Magn 2002; 38: 3039
- [26] Blázquez JS, Conde CF, Conde A, J Non-Cryst Solids 2001; 287: 187
- [27] Suzuki K, Cadogan JM, Dunlop JB, Sahajwalla V, Appl Phys Lett 1995; 67: 1369
- [28] Vogel H, Von Heimendahl M, Mat Sci Eng 1983; 57: 171
- [29] Lu K, Wang JT, J Mat Sci 1988; 23: 3001
- [30] Pratap A, Raval KG, Gupta A, Kulkarni SK, Bull Mat Sci 2000; 23: 185
- [31] Chen WZ, Ryder PL, Mat Sci Eng B 1995; 34: 204
- [32] Blázquez JS, Lozano-Pérez S, Conde A, Phil Mag Lett 2002; 82: 409

Figure captions

Figure 1. DSC scans at different heating rates for as-cast samples of the $\text{Fe}_{60}\text{Co}_{18}\text{Nb}_6\text{B}_{16}$ alloy.

Figure 2. Kissinger (above), Augis-Bennett (center) and Gao-Wang (below) plots for obtaining Q values for alloys with Cu (hollow symbols) and without Cu (solid symbols) with 18 (triangles), 39 (circles) and 60 at. % of Co (squares).

Figure 3. Comparison between the local values of Avrami exponent, $n(X)$, obtained for the $\text{Fe}_{60}\text{Co}_{18}\text{Nb}_6\text{B}_{16}$ alloy using different heating rates.

Figure 4. Local Avrami exponent, $n(X)$, obtained for the different alloys using 10 K/min as heating rate.

Figure 5. Local Avrami exponent, $n(X)$, obtained from expression (18) for different values of activation energy, $Q = 3$ (solid), 4 (dashed) and 5 (dotted), for the $\text{Fe}_{60}\text{Co}_{18}\text{Nb}_6\text{B}_{16}$ alloy heated at 20 K/min.

Figure 6. Local Avrami exponent, $n(T)$, obtained from the Ozawa method for the different studied alloys.

Figure 7. Comparison between the local Avrami exponent, $n(T)$, obtained from the Ozawa method and those obtained from (18) for each heating rate for the $\text{Fe}_{60}\text{Co}_{18}\text{Nb}_6\text{B}_{16}$ alloy.

Figure 8. Comparison between local values of Avrami exponent, $n(X)$, obtained from non-isothermal method, with constant activation energy (dotted), with a linear decrease of $Q(X)$ (bold solid line) and from isothermal results for two given temperatures [11].

Table I

Activation energies obtained by different methods.

Alloy	Kissinger [26] (eV) ± 0.2	Augis-Bennett (eV) ± 0.2	Gao-Wang (eV) ± 0.2
Fe ₆₀ Co ₁₈ Nb ₆ B ₁₅ Cu ₁	3.6	3.8	3.7
Fe ₃₉ Co ₃₉ Nb ₆ B ₁₅ Cu ₁	3.6	3.6	3.6
Fe ₁₈ Co ₆₀ Nb ₆ B ₁₅ Cu ₁	3.1	3.2	3.1
Fe ₆₀ Co ₁₈ Nb ₆ B ₁₆	3.9	4.4	4.4
Fe ₃₉ Co ₃₉ Nb ₆ B ₁₆	3.6	3.3	3.3
Fe ₁₈ Co ₆₀ Nb ₆ B ₁₆	3.5	3.4	3.4

Figure 1

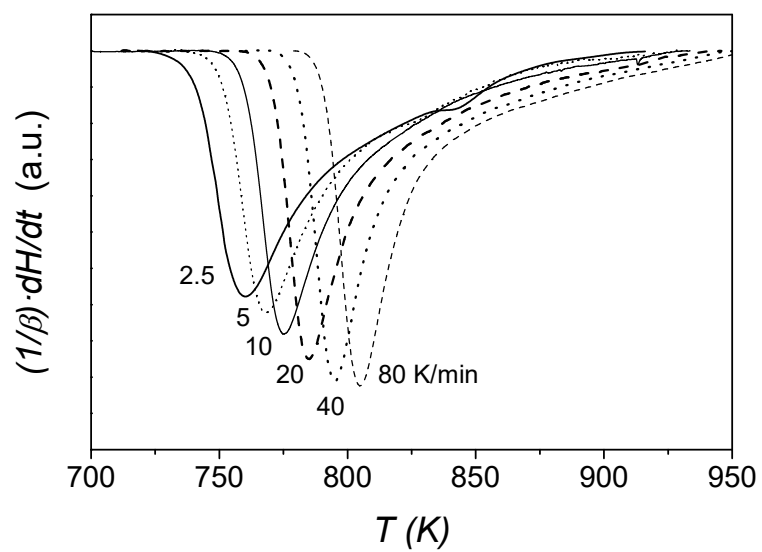


Figure 2

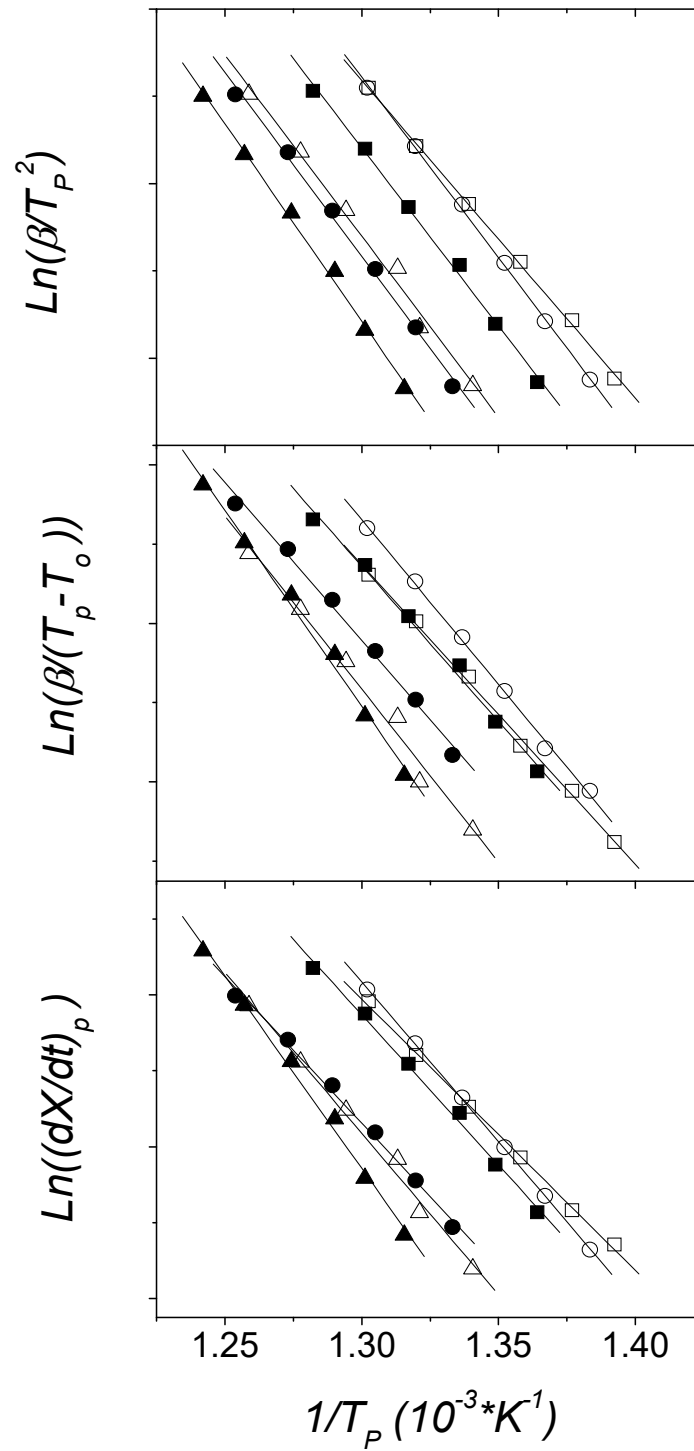


Figure 3

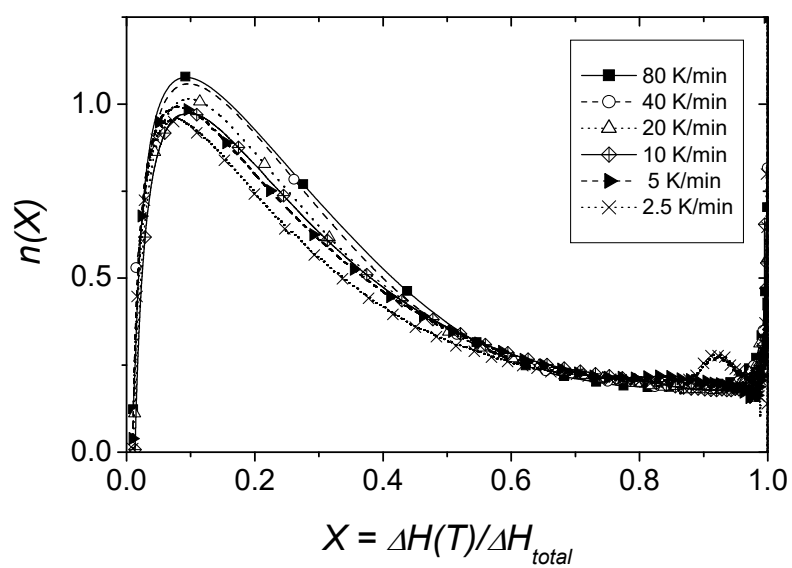


Figure 4

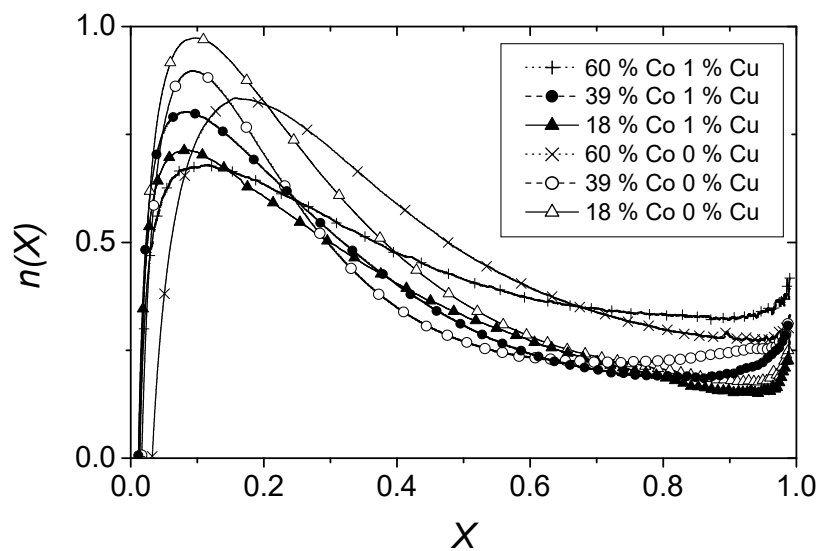


Figure 5

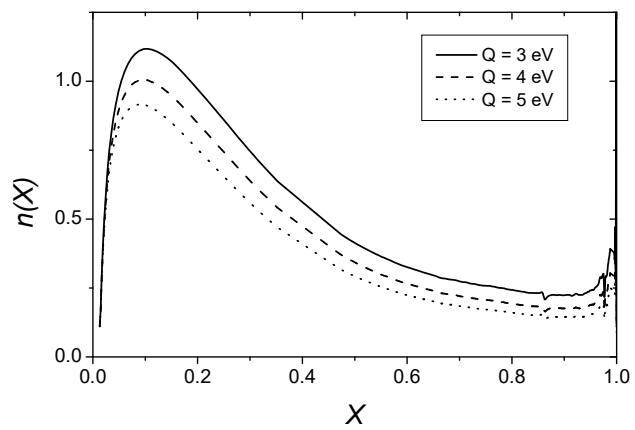


Figure 6

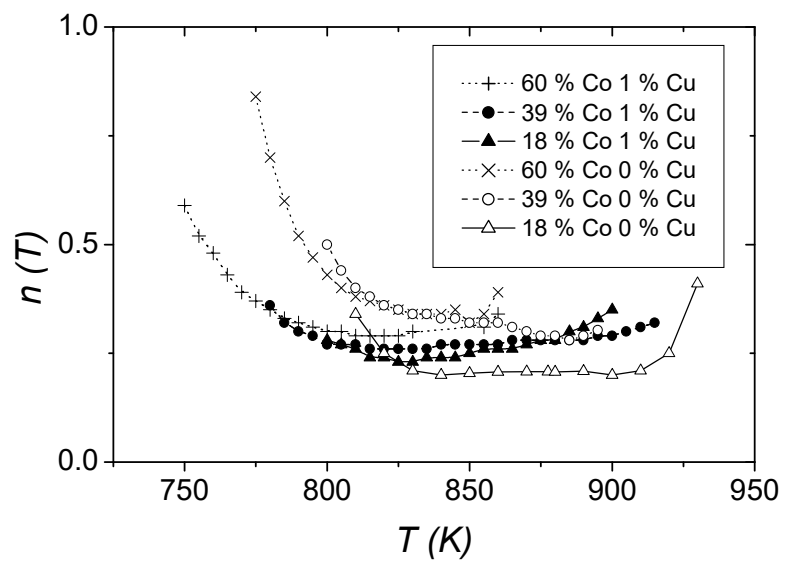


Figure 7

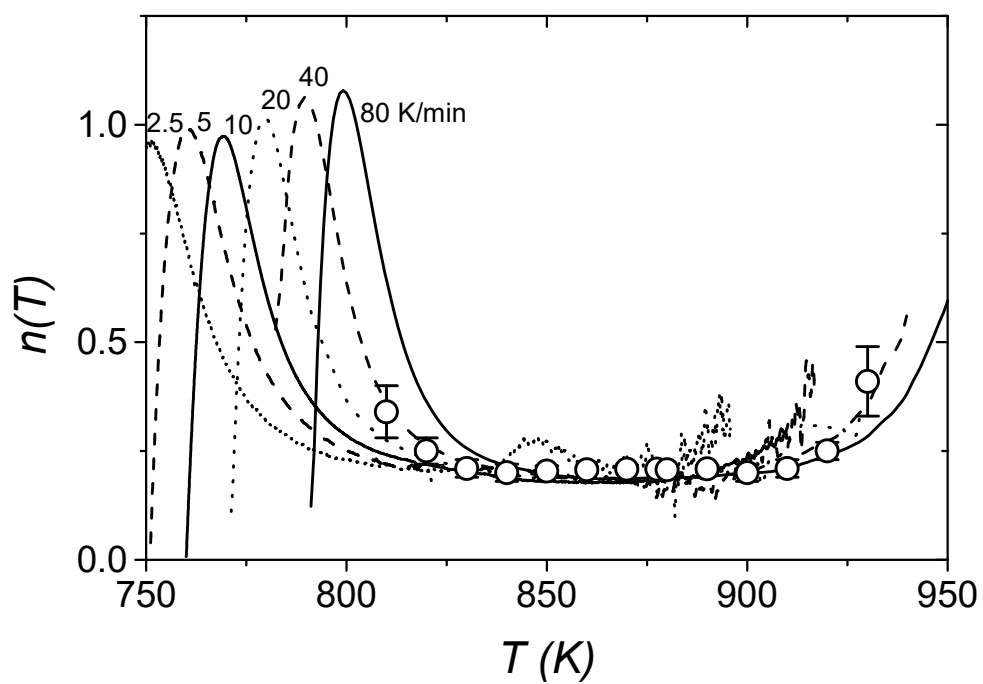


Figure 8

